2,3-Didehydro-1,4-benzoquinone. A quantum thermochemical study

Christopher J. Cramer

Department of Chemistry and Supercomputer Institute, University of Minnesota, 207 Pleasant St. SE, Minneapolis, MN 55455-0431, USA

Received (in Cambridge, UK) 19th April 1999, Accepted 21st May 1999

Correlated electronic structure calculations at single and multireference levels of theory have been carried out for several neutral and radical anion electronic states of 2,3-didehydro-1,4-benzoquinone, a quinone analog of *o*-benzyne. The molecule is predicted to be a ground-state singlet ($^1A_1$) with a 298 K heat of formation of 200.6 kJ mol^{-1}, a heat of hydrogenation (1 equiv.) of −323.5 kJ mol^{-1}, and an electron affinity of 1.95 eV; the latter quantity is in good agreement with an experimental value of 1.86 eV. The lowest energy triplet (1^3B_2), derived from an in-plane $\pi\rightarrow\pi^*$ excitation, is predicted to be 2.23 eV higher in energy than the singlet. The singlet and triplet states have biradical stabilization energies of 2.01 and −0.22 eV, respectively. Other triplet states derived from excitations involving the out-of-plane π system are also examined. A recent photoelectron spectrum of the radical anion is interpreted, and a poorly resolved feature is proposed to correspond to the singlet ($^1A_1$) ground state of 2,*6*-didehydro-1,4-benzoquinone. Technical aspects governing the suitability of various levels of theory are also discussed.

Didehydroarenes (often "arynes") have long been known to be reactive intermediates in various chemical transformations.[1–4] As a class, they show different degrees of biradical character depending upon the separation distance and relative orientation of the orbitals at the dehydro positions.[5] When the two positions are adjacent to one another, these molecules are additionally interesting to the extent that they incorporate bonds of order formally up to triple in small or medium rings. The best characterized examples are *o*-benzyne and some of its substituted derivatives, which have become common reagents for organic and organometallic synthesis.[1–4,6–8]

Davico *et al.*[9] have recently provided a variation on this theme; in particular, they measured the gas-phase negative ion photoelectron spectrum (NIPES) of the radical anion of 2,3-didehydro-1,4-benzoquinone (2,3-DDQ; benzoquinyne might be an acceptable short form, but will not be used here). This is a particularly interesting variation because, while it is superficially analogous to a benzenoid system, 1,4-benzoquinone itself would probably *not* be defined to be aromatic by most organic chemists. In spite of having a cyclic array of 6 p orbitals in a six-membered ring, each arguably contributing one electron to achieve a total number consistent with the Hückel $4n + 2$ rule, the situation is complicated by the carbonyl groups being cross-conjugated with the C=C double bonds. The simple exercise of drawing a Lewis structure for the molecule makes it clear that 1,4-benzoquinone has only a single "reasonable" resonance structure involving a six-membered ring formed from two C=C double bonds and four C–C single bonds. Amplifying on this point, 2,3-DDQ differs from *o*-benzyne not only by virtue of carrying substituent oxo groups that can exercise steric and electronic influences, but also by virtue of important geometric differences associated with bond localization before and after dehydrogenation, and in that sense the comparison between 2,3-DDQ and more typical arynes is of special interest.

The NIPES experiment of Davico *et al.*[9] shows two distinct features. The feature at lower energy exhibits extensive vibrational structure and, based on a detailed analysis of the vibrations and Franck–Condon intensities, was assigned by Davico *et al.*[9] as the closed-shell singlet ($^1A_1$) state of 2,3-DDQ. Further, the origin peak for this state was unambiguously assigned, indicating an electron affinity (EA) of 1.859 ± 0.005 eV for 2,3-DDQ. Davico *et al.*[9] compared this value to their own computations at the B3LYP/aug-cc-pVDZ level, which yielded a predicted EA of 2.44 eV, and pointed out that this error is considerably larger than would be expected based on literature reports[10] for many other EAs.

This surprising failure of a usually respectable level of theory is one factor motivating the present work. In addition, there remains an issue of the second feature observed in the NIPES experiment. This feature is broad and weak, with no discernible vibrational structure. In the absence of such structure, it is impossible to assign an origin, but the *center* of the feature is found at an electron binding energy of approximately 2.9 eV, *i.e.*, about 1 eV greater binding energy than is found for singlet 2,3-DDQ. Based on the asymmetry parameter β for photodetached electrons, Davico *et al.*[9] initially assigned this second feature to the triplet state of 2,3-DDQ analogous to the lowest energy triplet of *o*-benzyne ($^3B_2$ in each molecule). This would correspond to a singlet–triplet (S–T) splitting of *less* than 1 eV (since the unassigned origin must be at lower electron binding energy than the center of the feature), which is again substantially different from a prediction[9] of 1.9 eV at the B3LYP/aug-cc-pVDZ level. Of course, were the less than 1 eV S–T splitting to be correct, this would make the splitting in 2,3-DDQ considerably smaller than in *o*-benzyne, a somewhat surprising result insofar as the geometries of the parent systems would seem to favor a formal triple bond more in the quinoidal system than in the benzene system, which should then lead to a *larger* splitting. Further clarifying this situation was a second motivation for this work.

The goal of this paper, then, is to gain a clearer picture of the relative energies for various states of 2,3-DDQ, and moreover to better understand the thermochemical similarities and differences between 2,3-DDQ and *o*-benzyne. A secondary goal is to better characterize the strengths and limitations of different electronic structure methodologies applied to this problem. To that end, results are reported from density functional theory (DFT), multireference second-order perturbation theory (CASPT2), and single-reference coupled cluster (CCSD(T)) calculations, the latter level including single and double excitations to infinite order and a perturbative estimate of triple excitations.

Computational methods

Molecular geometries for all species were optimized at the

density functional level of electronic structure theory using the cc-pVDZ basis set.[11] DFT calculations employed the gradient-corrected functionals of Becke[12] and Perdew *et al.*[13] (BPW91). At this level, unrestricted calculations were carried out for all open-shell systems; for singlets 2,3-DDQ and 2,6-DDQ, broken-spin-symmetry SCF calculations invariably converged to the restricted DFT solution. All DFT geometries for 2,3-DDQ states were planar C_{2v} species confirmed, with the exception of one each high-energy triplet and radical anion, as local minima by computation of analytic vibrational frequencies—said frequencies were also used to compute zero-point vibrational energies (ZPVE) and thermal contributions to the 298 K enthalpies ($H_{298} - H_0$). Total spin expectation values for Slater determinants formed from the optimized (unrestricted) Kohn–Sham orbitals did not exceed 2.02 for the triplets nor 0.76 for the doublets.

At the BPW91 level, single point calculations using the aug-cc-pVDZ and cc-pVTZ basis sets[11] were also carried out for all structures (the former basis includes, on all atoms, diffuse functions of each angular momentum already present in the cc-pVDZ basis; the latter basis is valence-triple-ζ and includes polarization through f functions on second-row atoms and d functions on H). We define composite DFT energies as eqn. (1),

$$\text{Composite DFT} = \text{BPW91/cc-pVTZ//BPW91/cc-pVDZ} + [\text{BPW91/aug-cc-pVDZ//BPW91/cc-pVDZ} - \text{BPW91/cc-pVDZ}] \quad (1)$$

i.e., the effects of diffuse s, p, and d functions are evaluated for a valence-double-ζ basis set and then added to results from valence-triple-ζ calculations—such effects would be expected to be largest for the radical anions, where there is an "extra" electron, but might also be expected to be different for alternative electronic states where the number of electrons is the same but the degree to which they are tightly or loosely bound varies.

Molecular geometries were also optimized at the multi-configuration self-consistent field (MCSCF) level of theory for the singlet, triplet, and radical anion states of 2,3-DDQ. MCSCF/cc-pVDZ calculations were of the complete active space (CAS) variety and employed a 10-orbital active space comprised of the 8 π orbitals and the bonding and antibonding combinations of the in-plane dehydro σ orbitals; this space was occupied by either 10 electrons (the singlet and all triplet states) or 11 electrons (the radical anion states). Calculations using a still larger active space formed by adding one additional occupied and virtual orbital from each of the two irreducible representations spanning the σ orbitals (a_1 and b_2) were examined to evaluate the completeness of the 10-orbital active space. As the occupation numbers of the additional orbitals in these 14-electron/14-orbital wave functions either exceeded 1.99 (occupied) or were smaller than 0.01 (virtual) for the lowest energy singlet and triplet states, the 10-orbital active space was judged to be sufficient for the capture of non-dynamic correlation effects.

To improve the multireference calculations, dynamic electron correlation using the CAS reference was accounted for at the CASPT2N level[14–16] (hereafter called simply CASPT2) using the CAS/cc-pVDZ geometries. These calculations employed both the cc-pVDZ and aug-cc-pVDZ[11] basis sets. Some caution must be applied in interpreting the CASPT2 results, since this level of theory is known to sometimes suffer from a systematic error in the comparison of systems having different numbers of unpaired electrons.[15] For the singlet state and the lowest B_2 triplet state, CASPT2/cc-pVTZ calculations were also carried out. By analogy to eqn. (1), we define composite CASPT2 energies in eqn. (2).

$$\text{Composite CASPT2} = \text{CASPT2/cc-pVTZ//CAS/cc-pVDZ} + [\text{CASPT2/aug-cc-pVDZ//CAS/cc-pVDZ} - \text{CAS/cc-pVDZ}] \quad (2)$$

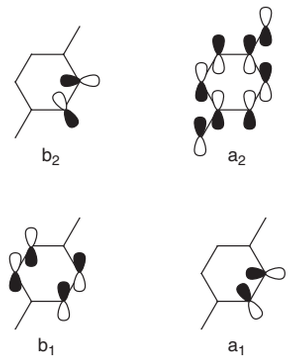

Fig. 1 The four orbitals whose various occupation numbers differentiate the electronic states of 2,3-DDQ and its radical anions. The out-of-plane π orbitals are shown here formally in the D_{2h} symmetry of *p*-benzoquinone itself, but inspection of the corresponding orbitals in 2,3-DDQ wave functions reveals that they are typically only very slightly perturbed by lowering the symmetry to C_{2v}. The in-plane π orbitals do mix with the remainder of the σ framework, but are dominated by the idealized representations shown here.

In addition, for the singlet, triplet, and radical anion states of 2,3-DDQ, single-reference Hartree–Fock wave functions were employed in CCSD(T)[17–20] and BCCD(T)[21] calculations (instead of HF orbitals, BCCD(T) uses Brueckner orbitals; these orbitals eliminate contributions from single excitations in the CC ansatz, which can reduce potential instabilities in the perturbative estimation of energetic effects associated with triple excitations when single excitation amplitudes in the HF-orbital-based method are large,[22] a situation previously observed in some aryne systems[23]). Energies were computed for both the BPW91 and CAS geometries. In most cases, these computations employed the cc-pVDZ basis set; for one case, the aug-cc-pVDZ basis was employed. Calculations at these levels using the cc-pVTZ basis set proved impractical.

CASPT2 and CCSD(T) calculations analogous to those described above were also carried out for certain related species discussed in more detail below.

Isotropic hyperfine coupling constants (hfs) were calculated by eqn. (3),[24] where g is the electronic g factor, β is the Bohr

$$a_X = (4\pi/3)\langle S_z\rangle^{-1} g g_X \beta \beta_X \rho(X) \quad (3)$$

magneton, g_X and β_X are the corresponding values for nucleus X, and ρ(X) is the Fermi contact integral, eqn. (4), where $\mathbf{P}^{\alpha-\beta}$

$$\rho(X) = \sum_{\mu\nu} P^{\alpha-\beta}_{\mu\nu} \varphi_\mu(\boldsymbol{R}_X)\varphi_\nu(\boldsymbol{R}_X) \quad (4)$$

is the BPW91/cc-pVDZ one-electron spin density matrix, and evaluation of the overlap between basis functions φ_μ and φ_ν is only at the nuclear position, $\boldsymbol{R}_X$. Dipole moments were computed as expectation values of the dipole moment operator.

Multireference and single-reference calculations were carried out with the MOLCAS[16] and GAUSSIAN94[25] electronic structure program suites, respectively.

Results

In 2,3-DDQ, the relatively small energy range spanned by the highest occupied π orbital of the quinone ring (which is of b_1 symmetry), the in-plane π and π* orbitals associated with the aryne (which are of a_1 and b_2 symmetry, respectively), and the lowest virtual π orbital of the quinone (which is of a_2 symmetry), suggests it might be possible for several different electronic states having similar energies to exist (Fig. 1). All of the seven 2,3-DDQ states discussed in this paper are formed from distributing the highest energy four electrons—or five in the case of the radical anions—amongst these four orbitals. Thus, the dominant configurations giving rise to the electronic states

discussed below are eqns. (5)–(11), where the natures of the states relative to the (ground-state) singlet have also been described in terms of electron attachments or excitations. For single-determinant theoretical methods (*e.g.*, DFT and Hartree–Fock) eqns. (5)–(11) describe the configurations

$$^2A_2^- = |\ \ldots b_1^2 a_1^2 a_2^1\rangle \quad (e^- \text{ attachment to out-of-plane } \pi^*) \quad (5)$$

$$^2B_2^- = |\ \ldots b_1^2 a_1^2 b_2^1\rangle \quad (e^- \text{ attachment to in-plane } \pi^*) \quad (6)$$

$$^1A_1 = |\ \ldots b_1^2 a_1^2\rangle \quad (7)$$

$$1^3B_2 = |\ \ldots b_1^2 a_1^1 b_2^1\rangle \quad (\text{in-plane } \pi \rightarrow \text{in-plane } \pi^*) \quad (8)$$

$$2^3B_2 = |\ \ldots b_1^1 a_1^2 a_2^1\rangle \quad (\text{out-of-plane } \pi \rightarrow \text{out-of-plane } \pi^*) \quad (9)$$

$$1^3A_2 = |\ \ldots b_1^1 a_1^2 b_2^1\rangle \quad (\text{out-of-plane } \pi \rightarrow \text{in-plane } \pi^*) \quad (10)$$

$$2^3A_2 = |\ \ldots b_1^2 a_1^1 a_2^1\rangle \quad (\text{in-plane } \pi \rightarrow \text{out-of-plane } \pi^*) \quad (11)$$

converged in the self-consistent field (SCF) process exactly. For CAS calculations, the configurations in eqns. (5)–(11) were the *dominant* configurations in the MCSCF wave functions.

Fig. 2 provides the optimized geometries from both the BPW91 and CAS levels for all of the 2,3-DDQ electronic states examined here. These species will hereafter be identified simply by their electronic state, as indicated in the figure. Fig. 3 provides BPW91 geometries for five other species considered here, namely *p*-benzoquinone singlet (Q) and radical anion (Q^-), dehydro-1,4-benzoquinone radical (DQ), and 2,6-didehydro-1,4-benzoquinone singlet (2,6-DDQ) and radical anion (2,6-DDQ^-). The state symmetries for these five species are ^1A_g, $^2B_{2g}^-$, $^2A'$, $^1A_1$ and $^2B_1^-$, respectively, but to avoid possible confusion with states of 2,3-DDQ these molecules will be referred to hereafter only by acronym. Fig. 3 also indicates the isotropic hyperfine splittings (hfs) computed for the protons in DQ. Previous studies have shown that these hfs constants can be used to accurately estimate the S–T splittings in the different diradicals that would be derived by the removal of corresponding hydrogen atoms, as discussed in more detail below.

Absolute and relative electronic energies, zero-point energies, and thermal enthalpic contributions for the two sets of molecules in Figs. 2 and 3 are provided in Tables 1 and 2, respectively, at various levels of theory. Large discrepancies are observed in some instances between different levels of theory; a discussion of technical aspects rationalizing these discrepancies is provided at the end of the Discussion section.

Representing a distillation from the copious theoretical numbers, Fig. 4 summarizes the key thermochemical quantities of interest associated with the 2,3-DDQ system. The details of how these best estimates were arrived at are provided in the next section. As part of that process, the applicability of various levels of theory for 2,3-DDQ was evaluated by examining the performance for analogous computations involving *o*-benzyne, for which experimental data for several thermochemical observables are available.[26] Table 3 contains the theoretical and experimental data for benzene, phenyl radical, *o*-benzyne, ethylene, and acetylene, required to make these comparisons.

Discussion

This section will focus first on the structure, bonding, and thermochemistry of 2,3-DDQ. For most of the discussion, I will make use of the best estimated values for various quantities tabulated in Fig. 4. A more detailed technical comparison between levels of theory, and in particular an analysis of the surprising failure of DFT to adequately represent certain states that do not suffer from high multideterminantal character, will follow.

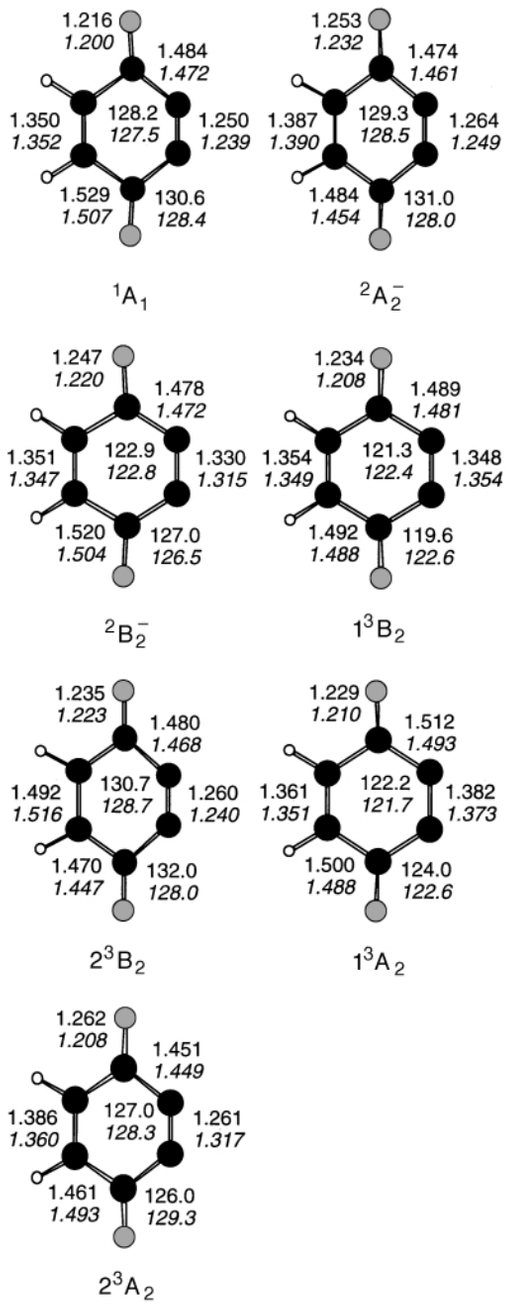

Fig. 2 Selected structural data for five neutral and two anionic states of 2,3-DDQ at the BPW91/cc-pVDZ (roman) and CAS/cc-pVDZ (italic) levels of theory. Bond lengths are in Å and bond angles are in deg.

Geometries

I begin by noting that for all four electronic states where CCSD(T) calculations were carried out for both the DFT and the CAS geometries, the DFT geometry was found to be lower in energy by from 0.6 to 2.5 kcal mol^{-1}. The better quality of DFT geometries compared to CAS has been observed in various aryne systems, to include even cases where the DFT energies are not particularly good.[23,26–33] This phenomenon is borne out in this study as well. As noted below, the stability of the $^2A_2^-$ state is badly overestimated at the DFT level; nevertheless the DFT geometry is 2.5 kcal mol^{-1} lower in energy at the CCSD(T) level than is the CAS geometry. For simplicity, most further discussion of geometries will focus only on the DFT predictions.

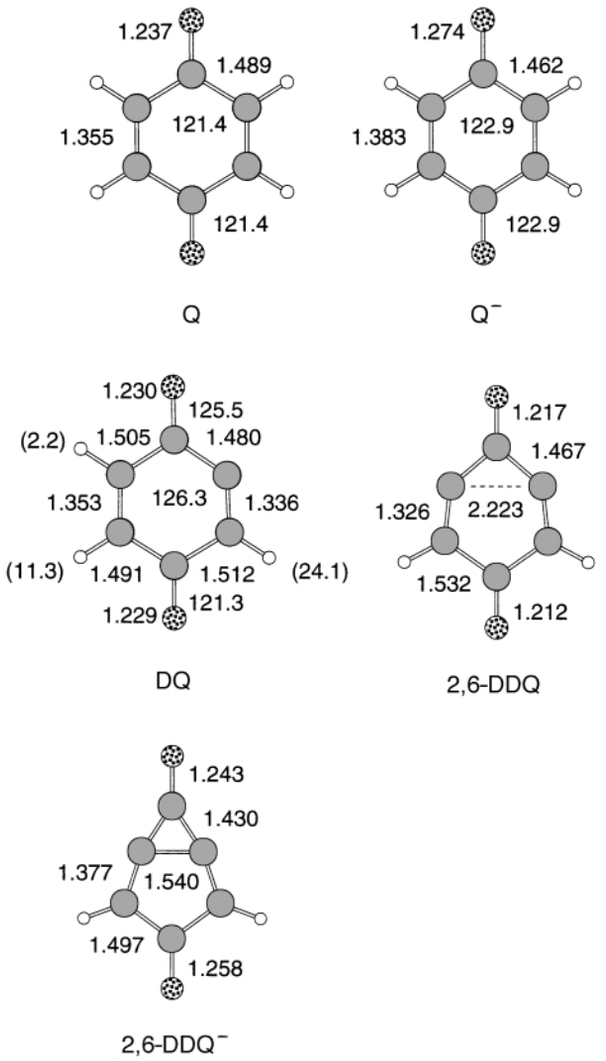

Fig. 3 Selected structural data for various molecules relevant to the study of 2,3-DDQ at the BPW91/cc-pVDZ level of theory. Bond lengths are in Å, bond angles are in deg, and ^{1}H hfs constants (in parentheses) are in G.

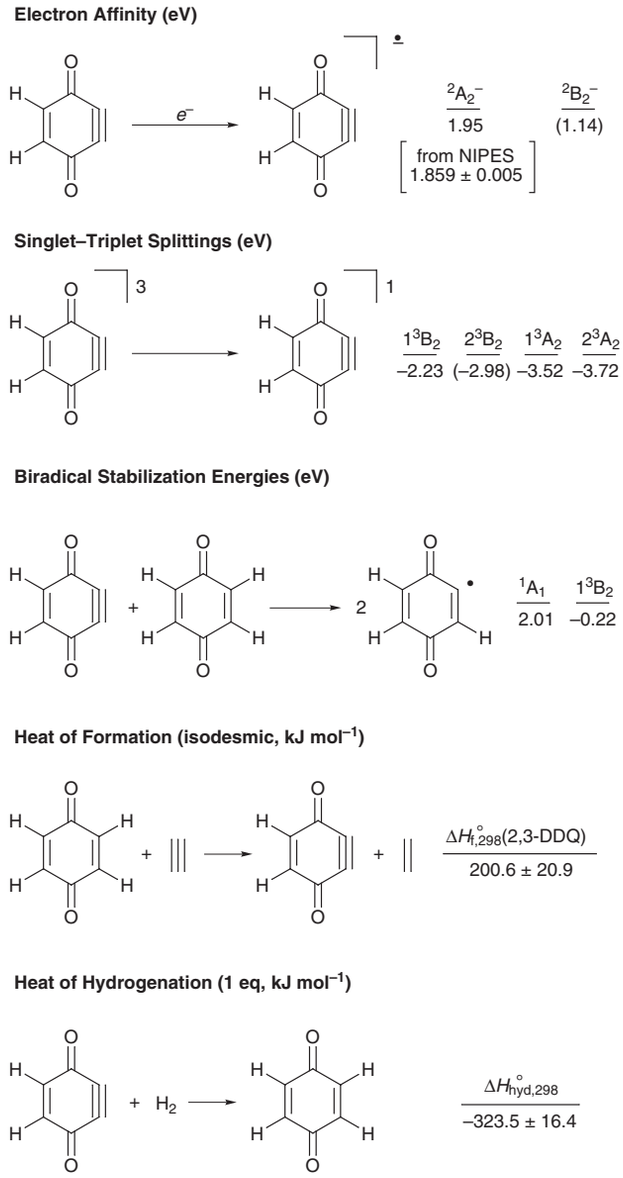

Fig. 4 Best estimates for selected thermochemical data involving 2,3-DDQ. See text for details on estimation procedures. Electron affinities and S–T splittings are H_0 and other quantities are H_{298}.

To begin, consider the change in geometry observed on going from parent Q to $^1A_1$ 2,3-DDQ. As expected, Q itself has substantial bond alternation in the six-membered ring, with the (H)C=C(H) bonds having lengths consistent with full double-bond character. On removal of two adjacent hydrogens, the affected bond shrinks 0.105 Å, consistent with a large degree of triple-bond character, while the other C=C bond length is essentially unaffected. The new biradical centers also show CCC valence bond angles increased from 121.4 to 128.2 deg, as they develop increased sp character. Interestingly, as discussed further below, the C=O bonds *also* shorten substantially, by 0.021 Å. This shortening derives from enhanced carbon s character in the C–O σ bond, which itself results from the CCO bond angle being 9.2 degrees wider in 2,3-DDQ—this rehybridization of the carbonyl carbons is driven primarily by the geometric requirements imposed on the ring by the presence of the formal triple bond. Thus, although Fig. 1 idealizes the a_1 and b_2 orbitals by localizing them entirely on the formal triple bond, it is evident that the actual orbitals have moderate localization on the carbonyl fragments too. The same carbonyl carbon rehybridization necessitates increasing p character to the remaining C–C bond, and indeed the (O)C–C(H) bond lengthens by 0.040 Å in $^1A_1$ compared to Q.

It is now instructive to consider the other electronic states of 2,3-DDQ as they derive from $^1A_1$. For instance, the lower-energy radical anions can be derived by attaching an electron to either the a_2 or b_2 orbitals. The former orbital is antibonding across the C=O, (H)C=C(H), and formal triple bonds, and one observes these bonds to increase in length by 0.037, 0.037, and 0.014 Å, respectively, in the $^2A_2^-$ state. The a_2 orbital is bonding, however, in a through-space sense between the two carbon atoms that are attached to each C=O group, and thus one observes the distance between these two carbons to decrease by 0.083 Å in $^2A_2^-$ (the "thinner" character of all of the 2,3-DDQ states in which the a_2 orbital is occupied is sufficiently large to be apparent even from casual inspection of Fig. 2). Creation of the $^2B_2^-$ state from electron attachment to the *in-plane* π* orbital, by contrast, substantially reduces triple bond character across the dehydro positions and thus gives rise as its main geometric consequence to a lengthening of that bond by 0.080 Å. In addition, the C=O bonds can be seen to noticeably bend away from that region of the molecule so as to decrease unfavorable Coulomb interactions between the negative charge density of the in-plane-localized anion and that surrounding the oxygen atoms.

The various triplet states are to a first approximation well represented by the configurations presented in eqns. (8)–(11), so again one can consider changes in geometry as being a function of which orbitals are depleted by one electron and which gain

Table 1 Energies (eV) for different electronic states of 2,3-DDQ relative to neutral singlet

Level of theory	Electronic state						
	$^1A_1$ [a]	$^2A_2^-$	$^2B_2^-$	1^3B_2	2^3B_2	1^3A_2	2^3A_2
BPW91/cc-pVDZ	0.00	−2.01	−0.84	1.94	2.30	3.23	1.70
BPW91/aug-cc-pVDZ [b]	0.00	−2.44	−1.35	1.93	2.26	3.19	1.72
BPW91/cc-pVTZ [b]	0.00	−2.24	−1.06	2.02	2.32	3.32	2.02
Composite DFT [c]	0.00	−2.67	−1.57	2.00	2.28	3.28	2.04
CAS/cc-pVDZ	0.00	0.34	0.72	2.00	2.77	3.53	5.48
CASPT2/cc-pVDZ [d]	0.00	−1.65	−0.63	1.88	2.53	3.19	3.47
CAS/aug-cc-pVDZ [d]	0.00	0.07	0.36	1.98	2.99	3.48	5.46
CASPT2/aug-cc-pVDZ [d]	0.00	−2.32	−1.35	1.84	2.52	3.11	3.33
CAS/cc-pVTZ [d]	0.00			2.05			
CASPT2/cc-pVTZ [d]	0.00			2.00			
Composite CASPT2 [e]	0.00			1.96			
CCSD/cc-pVDZ [b]	0.00	−1.32	−0.57	1.89	2.60		3.35
CCSD/cc-pVDZ [d]	0.00	−1.30		1.84	2.59	3.17	
CCSD(T)/cc-pVDZ [b]	0.00	−1.32	−0.48	2.07	2.73		2.06
CCSD(T)/cc-pVDZ [d]	0.00	−1.29		2.02	2.72	3.35	
CCSD/aug-cc-pVDZ [b]	0.00	−1.92					
BCCD/cc-pVDZ [b]	0.00			1.90			
BCCD(T)/cc-pVDZ [b]	0.00			2.06			
ZPVE [e]	0.00	−0.03	−0.06 [f]	−0.02	−0.08 [g]	0.00	−0.05
$H_{298} - H_0$ [b]	0.00	−0.01	−0.01	0.00	−0.01	−0.01	0.00

[a] Absolute energies for this column (h) are: −380.135 71, −380.158 69, −380.238 85, −380.261 83, −378.147 40, −379.079 97, −378.165 06, −379.144 35, −378.245 10, −379.427 50, −379.491 89, −379.103 22, −379.104 77, −379.158 08, −379.161 05, −379.166 16, −379.100 99, −379.160 14, 0.057 87, 0.006 50. [b] BPW91/cc-pVDZ geometry. [c] See eqn. (1). [d] CAS/cc-pVDZ geometry. [e] See eqn. (2). [f] Structure has an imaginary frequency of 142*i* cm^{-1}. [g] Structure has an imaginary frequency of 311*i* cm^{-1}.

Table 2 Absolute energies (h) for molecules in Fig. 3 and experimental data for Q

Level of theory	Q	Q$^-$	DQ	2,6-DDQ	2,6-DDQ$^-$
BPW91/cc-pVDZ	−381.445 02	−381.507 92	−380.763 50	−380.115 46	−380.203 45
BPW91/aug-cc-pVDZ [a]	−381.469 70	−381.548 25		−380.138 50	−380.240 11
BPW91/cc-pVTZ [a]	−381.550 23	−381.621 89		−380.217 12	−380.313 61
Composite DFT [b]	−381.574 91	−381.662 22		−380.240 16	−380.350 28
CAS/cc-pVDZ	−379.388 59		−378.736 15		
CASPT2/cc-pVDZ [c]	−380.377 84		−379.701 47		
CCSD/cc-pVDZ	−380.417 35				
CCSD(T)/cc-pVDZ	−380.466 87				
ZPVE [a]	0.082 47	0.080 73	0.069 32	0.056 07	0.056 00
$H_{298} - H_0$ [a]	0.006 39	0.006 18	0.006 48	0.005 83	0.006 20
Experimental data					
$\Delta H°_{f,298}$/kJ mol^{-1}	−122.9 ± 3.5 [d]				
EA/eV	1.912 ± 0.100 [e]				

[a] BPW91/cc-pVDZ geometry. [b] See eqn. (1). [c] CAS/cc-pVDZ geometry. [d] Ref. 40. [e] Ref. 36.

Table 3 Absolute energies (h) and experimental data for various hydrocarbons

Level of theory	Benzene	Phenyl radical	$^1A_1$ *o*-Benzyne	$^3B_2$ *o*-Benzyne	Ethylene	Acetylene
BPW91/cc-pVDZ	−232.229 46	−231.546 21	−230.902 76	−230.852 12	−78.574 57	−77.319 98
BPW91/aug-cc-pVDZ [a]			−230.913 25	−230.862 01		
BPW91/cc-pVTZ [a]			−230.964 73	−230.911 18		
Composite DFT [b]			−230.975 22	−230.921 07		
CAS/cc-pVDZ [c]	−230.794 31	−230.144 41	−229.542 25	−229.488 28	−78.067 93	−76.894 87
CASPT2/cc-pVDZ [d]	−231.504 70	−230.829 98	−230.195 45	−230.146 32	−78.318 53	−77.082 37
CCSD/cc-pVDZ [a]	−231.546 00	−230.861 23	−230.218 40	−230.173 77	−78.345 57	−77.099 24
CCSD(T)/cc-pVDZ [a]	−231.582 64	−230.897 09	−230.262 47	−230.209 74	−78.355 57	−77.110 70
ZPVE [a]	0.097 89	0.084 92	0.073 03	0.072 27	0.049 51	0.026 22
$H_{298} - H_0$ [a]	0.005 46	0.005 46	0.004 60	0.004 53	0.004 02	0.003 84
Experimental data						
S–T splitting (H_0)/eV			−1.626 ± 0.013			
BSE/kJ mol^{-1}			153.4 ± 14.2	−2.9 ± 14.2		
$\Delta H°_{f,298}$/kJ mol^{-1}	82 ± 0.7		442.7 ± 13.8	599.0 ± 13.8	52.5 ± 0.4	228.2 ± 0.7
$\Delta H°_{hyd,298}$ (1 equiv.)/kJ mol^{-1}			−360.1 ± 13.8			−175.7 ± 0.8

[a] BPW91/cc-pVDZ geometry. [b] See eqn. (1). [c] See Ref. 27 for active space details. [d] CAS/cc-pVDZ geometry.

one electron in comparison to the $^1A_1$ state. So, for the lowest energy triplet 1^3B_2, the transfer of an electron from the in-plane π to the in-plane π* effectively annihilates all triple-bond character, and the dehydro C=C bond length increases to within 0.007 Å of its value in Q. Indeed, this state has a geometry remarkably similar in all respects to that of Q. The 2^3B_2 state, on the other hand, is generated from changes in occupation of two *out-of-plane* π orbitals. In particular, the $b_1 \rightarrow a_2$ excitation reduces occupation of an orbital that is bonding across the CC multiple bonds and increases occupation of an orbital that is antibonding across these bonds. In the lower symmetry of 2,3-DDQ (compared to Q), this large increase in net antibonding π character is most manifest in the (H)C=C(H) bond, which lengthens by 0.142 Å compared to $^1A_1$. The formal triple bond lengthens also, but only by 0.010 Å. On the other hand, the $b_1 \rightarrow a_2$ excitation significantly *increases* the π *bonding* character between the two carbon atoms attached to each C=O group, so the distance between these two atoms in 2^3B_2 is 0.100 Å smaller than in $^1A_1$.

Generation of the 1^3A_2 state involves depopulating the *out-of-plane* orbital that is π-bonding across the formal triple bond, and populating the *in-plane* orbital that is π-*anti*bonding across that bond. Thus, compared to $^1A_1$, this bond becomes longer by fully 0.132 Å. A much smaller effect, an increase of 0.011 Å, is seen for the (H)C=C(H) double bond, since the b_2 orbital has almost zero amplitude across this connection.

Finally, the 2^3A_2 state shows rather curious behavior. Although it is the a_1 *in-plane* π-bonding orbital that is depopulated, and the a_2 *out-of-plane* π orbital (that is antibonding across the formal triple bond) that is occupied, there is evidently substantial orbital rehybridization that takes place in the triplet because the formal triple bond lengthens by only 0.011 Å compared to $^1A_1$. This DFT result stands in marked contrast to the CAS prediction, where the same bond is predicted to lengthen by a much larger 0.078 Å. Furthermore, at the DFT level, the C=O bonds lengthen by 0.046 Å, while at the CAS level, this increase is only 0.008 Å. It seems, then, that in the case of DFT the depletion of a_1 density is predominantly from the C–O σ bonds, and the localization of the a_2 orbital is also primarily across these bonds (in the antibonding sense indicated in Fig. 1). As discussed further below, these discrepancies are associated with a severe inaccuracy of DFT in describing this state. Because it is fairly challenging to coax a UHF wave function to converge for this state, I do not have a CCSD(T) energy for the CAS geometry, so it is impossible to judge which of the two geometries is better (again, I note that DFT can provide excellent geometries for states where its prediction of energies is quite poor). However, as also noted below, there are severe instabilities in the perturbative estimation of triples contributions to the coupled cluster energy for this state, so it seems unlikely that this level of theory would be adequate for judging the situation in any case. In the final analysis, in spite of being interesting because of the challenges it evidently poses for various theoretical methods, 2^3A_2 is too high in energy to be of much chemical relevance.

I conclude this sub-section with a brief digression to discuss the intriguing geometries of 2,*6*-DDQ and its radical anion. The 2,6-DDQ system obviously merits its own detailed study, but here I note simply that, like *m*-benzyne,[28,34] the *meta*-related naphthalynes,[35] and the *meta*-related pyridynes,[29] there is obviously a non-trivial bonding interaction between the two dehydrocarbons in the ground-state singlet. In the benzyne and pyridyne cases,[28,29,34] the potential of mean force associated with changing the distance between these two centers has been shown to be extraordinarily flat, and sensitive to such technical issues as whether or not broken-spin-symmetry determinants are employed in the DFT calculations. In contrast to *m*-benzyne and related systems, however, 2,6-DDQ^- formed from electron attachment to the neutral does *not* derive from occupation of the formal σ* *antibonding* orbital between the two dehydro centers, but instead from occupation of the π* orbital analogous to the a_2 orbital in 2,*3*-DDQ (because the symmetry axis in 2,6-DDQ is through the carbonyl groups instead of through the C=C multiple bonds, the π* orbital in question is b_1 in 2,6-DDQ). Recalling that this orbital is π-*bonding* between the two carbon atoms attached to the C=O groups, this nicely rationalizes why the radical anion is characterized by a single bond of 1.540 Å between the two dehydro centers, *i.e.*, the molecule is well described as the radical anion of 3,6-dioxobicyclo[3.1.0]hexa-1,4-diene.

I return now to the thermochemical data tabulated in Fig. 4.

Electron affinity

As the electron affinity of $^1A_1$ 2,3-DDQ has been unambiguously measured by Davico *et al.*[9] to be 1.859 ± 0.005 eV, it is possible to evaluate the predictive values of different levels of theory directly. The composite DFT level grossly overstabilizes the $^2A_2^-$ state, for reasons which are discussed further below, and as a result overestimates the electron affinity by 0.81 eV. This stands in marked contrast to the usual performance of DFT for EAs—Rienstra-Kiracofe *et al.* have shown errors in EAs on a large number of molecules to typically be less than 0.1 eV for functionals and basis sets of quality very similar to those employed here.[10]

The CASPT2 level is also unsatisfactory. With the aug-cc-pVDZ basis set, the EA is overestimated by 0.46 eV. More disturbing than the absolute magnitude of this error is the change in EA on going from the CAS to the CASPT2 level, 2.39 eV (at the CAS/aug-cc-pVDZ level, the EA is actually slightly negative!). So large a change in EA attributable to dynamical electron correlation is clearly ill-suited for treatment by second-order perturbation theory. Put more succinctly, one should exercise caution in comparing systems having different numbers of electrons at the CASPT2 level.

The CCSD/aug-cc-pVDZ level of theory, on the other hand, provides an excellent estimate of the electron affinity, and it is that number, corrected for ZPVE, that appears in Fig. 4 for the energy of attachment to generate $^2A_2^-$. Since the effect of triple excitations with the cc-pVDZ basis set is computed to be less than 0.01 eV, this number also represents a composite CCSD(T) energy analogous to the composite DFT and CASPT2 energies defined in eqns. (1) and (2) above. Of course, it would be nice to examine the convergence of this EA with respect to increasing the size of the valence space, but such calculations were not practical in this instance.

As for $^2B_2^-$, given the instabilities of the DFT and CASPT2 levels of theory, I have estimated the energy of this state by adding the energy difference between it and $^2A_2^-$ at the CCSD(T)/cc-pVDZ level (0.83 eV) to the attachment energy to form the $^2A_2^-$ state and then correcting for ZPVE. This is a rather crude estimate, particularly as the planar $^2B_2^-$ state is calculated to be a transition state with a small imaginary frequency. Additional efforts seem unwarranted, however, given the large separation that would almost certainly still exist following any additional optimization of the geometry of this state.

That being said, it is interesting to note the qualitative differences between 2,3-DDQ and *o*-benzyne with respect to electron attachment to generate these two states. The oxo substituents present in the quinone lower the energy of the *out-of-plane* a_2 π* orbital by a large amount compared to its level in *o*-benzyne, where the lowest energy virtual orbital is the *in-plane* b_2 π*. Interestingly, the EA of 2,3-DDQ is extremely close to that for Q itself, the latter being 1.91 eV.[36] The implication is that the *out-of-plane* a_2 π* orbital is energetically little perturbed by removal of the two *in-plane* hydrogen atoms and concomitant

formation of an *in-plane* π bond between the remaining two electrons.

The oxo substituents do, however, also influence the energy of the *in-plane* b_2 π* orbital. The 1.09 eV attachment energy to generate this state in 2,3-DDQ is considerably larger than the analogous EA of *o*-benzyne, 0.56 eV.[26] The greater stability of the 2,3-DDQ radical anion derives from inductive (as opposed to conjugative) partial charge localization onto oxygen. As already noted above, this has the geometric effect of lengthening the C=O bonds and bending them away from the didehydro region where the remainder of the negative charge is localized.

State energy splittings

To resolve ambiguities associated with the tentative assignment by Davico *et al.*[9] of a featureless NIPES band to the 1^3B_2 state, most of my effort was put into establishing the $^1A_1$–1^3B_2 splitting. At three levels that have been explored previously for the analogous splitting in *o*-benzyne,[27] namely BPW91/cc-pVDZ, CASPT2/cc-pVTZ, and CCSD(T)/cc-pVDZ//BPW91/cc-pVDZ, the $^1A_1$–1^3B_2 splitting (electronic energy only) is predicted to be −1.94, −1.88, and −2.07 eV, respectively. The trend in these numbers is quite similar to that seen for *o*-benzyne, *i.e.*, CCSD(T) predicts the largest splitting and CASPT2 the smallest. If one corrects these numbers using the errors in the analogous *o*-benzyne splittings[27] compared to experiment[26] (with differences in ZPVE removed from the experimental values), one derives predicted values for the $^1A_1$–1^3B_2 splitting (electronic energy only) in 2,3-DDQ of −2.28, −2.20, and −2.29, respectively—an excellent agreement between the three levels. Adding in differences in ZPVE and taking the average of these three values provides the number listed in Fig. 4, *i.e.*, −2.23 eV. Given the diabatic correlation between the relevant orbitals in the two cases, I consider using the correction factors obtained from *o*-benzyne for the 2,3-DDQ splitting to be well justified.

As a check on quality, I examined the convergence of the DFT and CASPT2 levels of theory with respect to basis set size. At the composite DFT and CASPT2 levels, respectively, the uncorrected energy differences between the two states increase to −2.00 and −1.96 eV, respectively. This small increase indicates that convergence with respect to basis set size is being approached in a manner consistent with the magnitude of the best estimate. I also checked the stability of the CCSD(T) method by carrying out BCCD(T)/cc-pVDZ calculations for the two states. The two coupled-cluster approaches, differing in the nature of the orbitals used to express the reference wave function, provide identical results for the splitting to within 0.01 eV, suggesting that neither spin state suffers from instabilities owing to large singles amplitudes that might[23] reduce the accuracy of the CCSD(T) computation. While no error bar is provided on the splitting in Fig. 4, a conservative estimate would probably be ±0.2 eV. As discussed further below, a splitting in excess of −1.5 eV would not allow the state to be seen in the NIPES experiment of Davico *et al.*[9]

As a final check, Cramer and Squires have reported that CASPT2/cc-pVDZ S–T splittings in biradicals correlate remarkably well with BPW91/cc-pVDZ monoradical ^{1}H hfs constants, where the hfs is computed for the hydrogen atom on the biradical site that is "capped" in the monoradical (while it is assumed that the correlation with experiment might be of similarly high quality, there are insufficient experimental data to correlate). For *ortho*- and *meta*-related biradicals, the regression equation, which has an *R* value of 0.997 when computed over relevant benzynes,[37] pyridynes,[29] and naphthalynes,[35,37] is eqn. (12). The computed hfs of 24.1 G for the *ortho* hydrogen atom

$$(\text{S–T splitting, eV}) = -0.0604 \times (^1\text{H hfs, G}) - 0.4112 \quad (12)$$

in DQ predicts a CASPT2 splitting of −1.86 eV, in almost perfect agreement with the actual CASPT2/cc-pVDZ value of −1.88 eV. This suggests that the CASPT2 description of the 2,3-DDQ biradical is very similar to related aryne biradicals and is interpretable along those lines.

With respect to the other state energies, I took a somewhat less rigorous approach to estimating their energies. In particular for 2^3B_2 and 1^3A_2, I considered the differences in electronic energies between these higher energy triplets and 1^3B_2 at the composite DFT, CASPT2/aug-cc-pVDZ, and CCSD(T)/cc-pVDZ levels (for the latter level of theory, difficulties in convergence necessitated use of the CAS geometry instead of the DFT geometry for the 1^3A_2 state, but this is not expected to make much difference given the close similarities in splittings for all other states as a function of geometries). These differences were then added to the best estimate (−2.26 eV after removal of ZPVE) for the $^1A_1$–1^3B_2 splitting to arrive at the $^1A_1$–2^3B_2 and $^1A_1$–1^3A_2 splittings. For the 2^3B_2 state, the predictions at the three levels are −2.53, −2.93, and −2.92 eV, respectively. Because DFT seems to perform poorly when the a_2 π* orbital is occupied (*vide infra*), only the latter two numbers were averaged, then augmented with ZPVE, to give the number reported in Fig. 4, −2.98 eV. Note that this state has one imaginary frequency when planar, suggesting that pyramidalization, probably to create a state resembling two triplet coupled ketyls, would lower the energy somewhat. It seems quite doubtful, however, that this lowering would invert its position relative to 1^3B_2, so no further studies were carried out to find the actual minimum. In the case of 1^3A_2, the above described levels of theory predict the $^1A_1$–1^3A_2 splitting (electronic energy only) to be −3.53, −3.52, and −3.59 eV, respectively. The close agreement between all three levels indicates that this state is well described by all of the different approaches. Averaging over these values and adding ZPVE gives the reported best estimate of −3.52 eV for this splitting.

The 2^3A_2 state is significantly more difficult to handle, with DFT and CCSD(T) both suffering severely from intrinsic deficiencies in their theoretical ansatzes when attempting to describe this state. The failures of the former level are discussed in more detail below. The latter level fails because very large singles amplitudes appear in the CCSD wave function and these make the triples estimation unreliable (hence the enormous change in relative energy on going from CCSD to CCSD(T)). For this state, a best estimate was derived by considering the average of the differences between the electronic energies of 2^3A_2 and 1^3B_2 at the CASPT2/aug-cc-pVDZ and BCCD/cc-pVDZ levels of theory (at the BCCD(T) level, in spite of using Brueckner orbitals, the perturbative estimation of triples contributions seems unreliably large). Both of these levels appear reasonably robust for this difference, and they predict the resulting $^1A_1$–2^3A_2 splitting (electronic energy only) to be −3.75 and −3.63 eV, respectively. The average of these two values, together with ZPVE differences, provides the splitting listed in Fig. 4, −3.72 eV.

Recalling the dominant configurations making up these various triplet states, it is evident that the lowest energy excitation from ground-state $^1A_1$ is the same *in-plane* π to *in-plane* π* found for *o*-benzyne. However, the energy required to access the triplet state is much lower for *o*-benzyne (1.626 ± 0.013 eV)[26] than for 2,3-DDQ. Most of this variation can be attributed to the difference in the aromatic characters of the two systems and the influence this has on their geometries. For *o*-benzyne in the singlet state, bond shortening increases the π overlap between the adjacent dehydro positions only at the expense of imposing a bond-alternating structure on the ring, which reduces the energetic stabilization associated with aromaticity. In 2,3-DDQ, on the other hand, aromaticity is not a factor, and strong localization of the formal triple bond is opposed only by ring strain, which of course is an effect operative in *o*-benzyne as well. There is also some differentiation between the triplet states in the two systems. The structure of the quinoidal system

enforces a smaller distance between the two dehydro centers, and hence generates more exchange-repulsion in 2,3-DDQ than in *o*-benzyne. These two effects, greater and lesser relative stability of the singlet and triplet, respectively, operate in concert to increase the size of the S–T splitting in 2,3-DDQ compared to *o*-benzyne.

With respect to accessing the higher energy triplets of 2,3-DDQ, the *out-of-plane* π to *out-of-plane* π* excitation to generate 2^3B_2 is predicted to require roughly 0.7 eV more energy than is required for the *in-plane* π to *in-plane* π* process just discussed. Energies for states derived from excitations involving one *in-plane* and one *out-of-plane* orbital are another 0.7 eV higher still, with the difference between the two $^3A_2$ states sufficiently small that, within the errors in the theory, there is little preference for the direction of the excitation. Since the *in-plane* and *out-of-plane* π systems are localized in different regions of space, the higher energy of the $^3A_2$ states derives in part from the charge separation required to generate them. This is most apparent in 1^3A_2, where the shift in electron density is from the b_1 orbital, which is centrally localized with respect to the atomic positions, to the b_2 orbital, which is localized exocyclic to the dehydro positions. This movement of charge is parallel to the dipole moment already present in the $^1A_1$ state (1.8 and 2.4 D at the CAS and DFT levels, respectively), and thus the dipole moment of the triplet is increased. Indeed, 1^3A_2 has the largest dipole moment of all of the 2,3-DDQ states, namely 2.7 and 3.4 D at the CAS and DFT levels, respectively, which represents an increase of about 1 D at both levels.

Movement of charge in 2^3A_2, on the other hand, is primarily from the dehydro region to the oxygen atoms. Such charge separation should manifest itself in a larger quadrupole moment, but this moment is origin-dependent for 2,3-DDQ, so a quantitative comparison is not here undertaken.

Biradical stabilization energies

Squires and co-workers[38,39] have emphasized the utility of analyzing the relative thermodynamic stabilities of biradicals by considering the enthalpy changes for isodesmic hydrogen transfer reactions from a dihydrogenated species to a biradical so as to give a pair of monoradicals. These changes are termed biradical stabilization energies (BSEs), as they provide a direct indication of the stabilization (BSE > 0) or destabilization (BSE < 0) that derives from both radical sites being present in the same molecule. Predicted BSEs have been reported for the benzynes[27,38] (where experimental[26] values are also available), α,*n*-didehydrotoluenes,[39] naphthalynes,[35] and pyridynes.[29]

In the case of 2,3-DDQ, the relevant isodesmic equation involves Q and DQ (Fig. 4). BSE values (298 K enthalpies) were computed for $^1A_1$ and 1^3B_2 using the data in Tables 1 and 2. At the DFT and CASPT2 levels, the predicted BSEs for $^1A_1$ are 1.42 and 1.45 eV, respectively, while for 1^3B_2 the predicted BSEs are −0.50 and −0.41 eV, respectively. At these same two levels of theory, the analogous isodesmic equation for *o*-benzyne yields BSEs of 1.05 and 1.06 eV, respectively ($^1A_1$) and −0.30 and −0.25, respectively ($^3B_2$); the measured BSEs for these two states are 1.59 and −0.03 eV, respectively.[26] To arrive at best estimates for 2,3-DDQ, I first correct the DFT and CASPT2 predictions by the errors these levels of theory exhibit for *o*-benzyne. This correction gives singlet and triplet BSEs of 1.97 and −0.22 eV, respectively. These numbers are then scaled so that the difference in the BSEs matches the 298 K S–T splitting (as it should), providing final estimates of 2.01 and −0.22 eV, respectively (Fig. 4). As a technical point, although CCSD(T) BSEs proved to be more accurate than DFT or CASPT2 in the benzynes,[27] they are not expected to be as useful here because the unrestricted Hartree–Fock reference wave function for the DQ radical is very badly spin-contaminated ($\langle S^2 \rangle = 1.891$; an expectation value of 0.750 is correct for a doublet).

As already noted above, the S–T splitting in 2,3-DDQ is larger than it is in *o*-benzyne. The BSE calculations provide a means of quantifying the degree to which this increase partitions between differences associated with the singlet *vs.* the triplet states. Comparing the 2,3-DDQ BSE best estimates to the experimental BSEs for *o*-benzyne, one sees that roughly two thirds of the predicted increase in the S–T splitting for 2,3-DDQ derives from enhanced stabilization of the singlet, while one third derives from greater destabilization of the triplet.

While the reaction from which the 2,3-DDQ BSEs are computed is isodesmic, the heat of formation of monoradical DQ is not known experimentally. Thus, this reaction cannot be used to compute a heat of formation for ground-state singlet 2,3-DDQ. I now describe an alternative approach to that computation.

Heat of formation of 2,3-DDQ

Gas-phase 298 K heats of formation have been measured for Q, acetylene, and ethylene.[40] Thus, all of the data necessary to estimate the heat of formation of 2,3-DDQ using the second isodesmic reaction shown in Fig. 4 are available. Moreover, if Q and $^1A_1$ are replaced with benzene and *o*-benzyne, respectively, the analogous isodesmic equation has been shown[27] to yield good predictions for the heat of formation of *o*-benzyne at a variety of levels of electronic structure theory, including those used here. To arrive at the 2,3-DDQ 298 K heat of formation reported in Fig. 4, I have evaluated the indicated isodesmic reaction at the BPW91/cc-pVDZ, CASPT2/cc-pVDZ, and CCSD(T)/cc-pVDZ//BPW91/cc-pVDZ levels. Each of these levels of theory was also employed to compute the 298 K heat of formation for *o*-benzyne using the analogous isodesmic reaction.[27] Correcting each level of theory as applied to $^1A_1$ 2,3-DDQ by the amount needed to bring that level into quantitative agreement with experiment[26] for *o*-benzyne (these corrections being 1.1, 3.7, and 9.5 kJ mol^{-1}, respectively) gives predicted heats of formation of 192.7, 208.4, and 200.7 kJ mol^{-1}, respectively. The value quoted in Fig. 3 represents the mean of these three calculations; the error bar is computed as the root-mean-square of the span of the computed values and the experimental error[26] in the heat of formation of *o*-benzyne.

Heat of hydrogenation of 2,3-DDQ

Since the heat of formation of dihydrogen gas is defined to be zero, the 298 K heat of hydrogenation of the *in-plane* π component of the triple bond in $^1A_1$ is simply the difference in the 298 K heats of formation of $^1A_1$ and Q. This value, −323.5 ± 16.4 kJ mol^{-1}, is a measure of the strength of the *in-plane* π bond (Fig. 4; the error is the root-mean-square of the estimated and experimental[40] errors for heats of formation of $^1A_1$ 2,3-DDQ and Q, respectively). If one carries out the same analysis using experimental heats of formation for benzene[40] and *o*-benzyne[26] and for acetylene[40] and ethylene,[40] one determines heats of hydrogenation of −360.5 ± 13.8 and −175.7 ± 0.8 kJ mol^{-1}, respectively. Thus, while the *in-plane* π component of the triple bond in $^1A_1$ is stronger than in *o*-benzyne, presumably because of the shorter length of the formal C–C triple bond, the additional stability is still substantially less than that found in the parent acetylene, where favorable overlap is not opposed by ring-strain constraints. (To be more fair a comparison, one might consider differences between acetylene and hex-3-yn-2,5-dione for the reference hydrogenation, but I am unaware of the availability of relevant experimental data, and I suspect the qualitative picture would not change.)

2,6-DDQ

In addition to the singlet 2,3-DDQ feature already described, the NIPES spectrum of Davico *et al.*[9] shows a weak, broad feature having its intensity maximum at an electron binding energy of approximately 2.83 eV; that is, about 1 eV higher in

energy than the (0,0) peak for $^1A_1$. As there is no discernible vibrational structure, it is possible neither to assign a (0,0) peak to the higher energy emission nor even to guess at roughly where it might be. Originally, this band was attributed to 1^3B_2 2,3-DDQ.[9] However, as shown above, 1^3B_2 is 2.2 eV higher in energy than $^1A_1$, and thus is well outside the detection range available in the Davico *et al.*[9] experiment, where photons having 3.4 eV of energy are used to ionize the negative ions. So, if the high-energy feature cannot be assigned to the 1^3B_2 state of 2,3-DDQ, to what can it be ascribed?

A possible clue lies in the analogous NIPES spectrum of *o*-benzyne. This species is generated in the gas phase by reacting benzene with O^-. Although 1,2-hydrogen-atom abstraction/electron transfer generates *o*-benzyne radical anion as a predominant product, it is always found to be contaminated with a certain amount of *m*-benzyne radical anion resulting from a 1,3-hydrogen-atom abstraction/electron transfer.[26] The analogy to this latter process when O^- is reacted with Q would generate 2,6-DDQ$^-$. This species and its neutral singlet have been described above in terms of their fascinating geometries. More germane to the NIPES experiment, however, at the composite DFT level, 2,6-DDQ is predicted to have an EA of 2.99 eV. Noting the overestimation of the analogous EA in 2,3-DDQ at this level, and noting the similar character of the SOMOs in the respective radical anions, it seems quite reasonable to assign the feature centered about 2.85 eV to 2,6-DDQ. This assignment is strengthened by the large difference in geometries for 2,6-DDQ and 2,6-DDQ$^-$: poor Franck–Condon overlap is consistent with the weak, broad nature of the feature.

However, the proposed assignment is *not* consistent with the interpretation offered by Davico *et al.*[9] of the asymmetry parameter β of the photoejected electrons. More quantitative support for the theoretical assignment will obviously require a much more complete study of 2,6-DDQ, which is not undertaken here. As a brief diversion, however, the proton hfs values listed in Fig. 3 can be used to estimate the S–T splitting in 2,6-DDQ. Using eqn. (12), the $^1A_1$–$^3B_2$ splitting in 2,6-DDQ is predicted to be −1.09 eV. Recalling that this prediction actually corresponds to an expected energy predicted at the CASPT2/cc-pVDZ level, a better estimate is probably arrived at by correcting this number for the error observed between the CASPT2 level and experiment[26] for *m*-benzyne—that error, exclusive of ZPVE, is 0.13 eV.[27] This correction provides a best estimate of −1.22 eV (I have not computed ZPVE differences for 2,6-DDQ, but ZPVE differences in *m*-benzyne are only 0.02 eV). The 2,6-DDQ $^3B_2$ state also lies significantly outside the window of the Davico *et al.* NIPES experiment,[9] so the quality of this prediction cannot yet be evaluated.

Finally, for the sake of completeness, the remaining hfs constant in Fig. 3 can be used to estimate the ^1A–^3B splitting in 2,5-DDQ—a species that has not yet been reported to have been generated, even accidentally. In the case of biradical centers not *ortho*- or *meta*-related, the correlating equation ($R = 0.987$) analogous to eqn. (12) is given by eqn. (13). Unlike eqn. (12),

$$(\text{S–T splitting, eV}) = -0.0864 \times (^1\text{H hfs, G}) - 0.0130 \quad (13)$$

which parametrically accounts for typically large geometry differences between the singlet, triplet, and doublet states of *ortho* and *meta* biradicals, eqn. (13) has a near-zero intercept, which meets with qualitative expectations that if a proton does not feel any unpaired electron spin density, an electron localized in the same position would not be expected to show much preference for singlet *vs.* triplet coupling. In any case, the predicted CASPT2/cc-pVDZ splitting for 2,5-DDQ is −0.20 eV. This is identical to the CASPT2/cc-pVDZ splitting predicted for *p*-benzyne,[23,27] where a measurement of −0.16 eV has been provided,[26] so that same value now serves as the best estimate for 2,5-DDQ.

Methodological issues

The remainder of this section, of interest primarily to electronic structure specialists, is devoted to an analysis of the failures of certain levels of theory—sometimes rather spectacular failures—for various species in this study.

The single most notable deficiency is the apparent inability of DFT to properly handle 2,3-DDQ electronic states when the *out-of-plane* π^* a_2 orbital is singly occupied. Such states are computed to be far too low in energy relative to states where this orbital is empty. Thus, at the composite DFT level, the EA of 2,3-DDQ is overestimated by 0.8 eV, and the energies of the 2^3B_2 and 2^3A_2 states relative to $^1A_1$ are predicted to be too low by 0.4 and 1.4 eV, respectively. This problem is *not* entirely dependent on the presence of the biradical, although it seems to be exacerbated by that presence. Thus, the BPW91/cc-pVDZ level (including ZPVE) predicts the EA of Q itself to be 2.42 eV, this being an overestimation of 0.51 eV compared to experiment.[36]

The error appears to derive from an overstabilization of states that can more readily transfer π electronic charge to oxygen. Since the two oxygen p_z orbitals contribute significantly to the out-of-plane π^* a_2 orbital, this effect is most manifest in cases where the a_2 orbital is occupied. However, the effect is particularly dramatic for 2^3A_2, where the DFT "wave function" appears to trade oxygen σ density for π density. That is, as already noted above, the geometry of this state suggests that the C–C triple bond in the ring is largely preserved, and that instead the loss of density from the σ framework is taken primarily from the C–O double bonds. This is best observed in the ^{17}O hfs value predicted for this state at the BPW91/cc-pVDZ level, 10.6 G. This very large oxygen hfs is not observed unless both the a_1 *and* a_2 orbitals are singly occupied. Thus, in 2^3B_2, where the a_2 orbital is singly occupied but the a_1 is not, the predicted ^{17}O hfs is only 1.8 G (a small number is expected since the oxygen atoms are in the nodal planes of the singly occupied orbitals). In 1^3B_2, where the a_1 orbital is singly occupied but the a_2 is not, the predicted ^{17}O hfs is 4.7 G, indicating that occupation of the a_2 orbital does shift significantly more spin density onto oxygen. This overpolarization of the electron density in certain states is reminiscent of the severe errors reported for DFT by Ruiz *et al.*[41] for various van der Waals complexes where anomalous charge transfer is observed to occur, but in 2,3-DDQ there are clearly subtleties associated with the nature of the orbitals themselves. It seems likely that this behavior is related to the increase in the electron self-interaction error noted for DFT in systems involving fractional numbers of electrons,[42] such systems being analogous to highly delocalized species.

In fairness, one should perhaps not *expect* DFT to do well with the 2^3A_2 and 2^3B_2 states. The Hohenberg–Kohn theorem[43] has not been proven to apply to states other than the ground state (or, more accurately, other than the lowest-energy state belonging to each irreducible representation of the molecular point group[44]). In practice, however, I have found DFT in many instances to do well with relative state energies not covered by the Hohenberg–Kohn theorem.[29,35,37,45,46] Moreover, $^2A_2^-$ and Q^-, which are computed to bind their extra electron too tightly, *are* ground states. So, there is clearly something special about the quinone system and the a_2 orbital that may merit future study, particularly by those developing improved density functionals.

The issue of the validity of describing excited states using a single-reference method arises for the CCSD(T) calculations as well, since they employ HF reference wave functions. For the 2,3-DDQ triplets, however, this level of theory seems to be reasonably robust even for 2^3A_2 and 2^3B_2. In the case of 2^3B_2, the predicted separation between this state and 1^3B_2, 0.67 eV, compares very favorably with the separation predicted at the CASPT2/cc-pVDZ level, 0.65 eV. This analysis is complicated for 2^3A_2 because large singles amplitudes make the CCSD(T)

triples estimation unreliable. However, if we compare the CCSD/cc-pVDZ difference in energies (no triples) between 2^3A_2 and 1^3B_2 (1.46 eV) to the CASPT2/cc-pVDZ difference (1.59 eV), there is quite reasonable agreement. Thus, provided the single determinants are qualitatively different by a margin as large as that observed between the different A_2 and B_2 triplets here, where alternative pairs of orbitals are singly occupied, the single-reference CCSD(T) method appears to have some utility for comparing different states having the same overall electronic symmetry. Recourse to more rigorous excited-state CCSD(T) methods[47] is preferred for problematic cases.

Finally, certain technical details associated with the CAS calculations merit some discussion. At the CAS/cc-pVDZ level, each triplet dominated by the configurations listed in eqns. (5)–(11) is predicted to be the lowest-energy root of the configuration interaction (CI) matrix at their respective geometries. Root switching problems during geometry optimizations were not observed. However, at the CAS/aug-cc-pVDZ level, 2^3A_2 is predicted to be the *second* root of the CI matrix, even at its CAS/cc-pVDZ optimized geometry and using orbitals *optimized* for this root. The absolute weights of configurations 10 and 11 in the CAS/aug-cc-pVDZ wave functions of 1^3A_2 and 2^3A_2 obtained under the latter set of conditions were 0.59/0.23 and 0.23/0.63, respectively, indicating substantial mixing of the two configurations in both states. Similarly, while at the CAS/aug-cc-pVDZ level 2^3B_2 is predicted to be the lowest energy root at its CAS/cc-pVDZ optimized geometry, converging the MCSCF equations with the augmented basis set did require optimizing the orbitals for the 50 : 50 mix of the two $^3B_2$ states, with the subsequent CASPT2 calculation being done only for the lower energy root. While these technical challenges require careful attention, and are thus noted here, they do not appear to adversely affect the trustworthiness of the CASPT2 model. I conclude by noting that at the CASPT2/aug-cc-pVDZ level, the weight of the reference CAS wave functions in the CASPT2 expansions varied only over the reasonably narrow range of 71.5 to 75.7%.

Conclusions

By evaluating results from three different levels of correlated electronic structure theory, I have developed estimates for several thermochemical observables associated with different didehydro-1,4-benzoquinones. In good agreement with experimental results from negative ion photoelectron spectroscopy, 2,3-didehydro-1,4-benzoquinone is predicted to be a ground-state singlet with an electron affinity of 1.95 eV. A second feature observed in the NIPES experiment is suggested to be the *meta*-related biradical 2,6-didehydro-1,4-benzoquinone. The 298 K heat of formation of 2,3-DDQ is predicted to be 200.6 kJ mol^{-1}, and the $^1A_1$–$^3B_2$ splitting is predicted to be 2.23 eV. The triplet state derives from an in-plane $\pi\rightarrow\pi^*$ excitation, and in this sense 2,3-DDQ and *o*-benzyne are analogous. The π interaction energy between the two dehydro centers in 2,3-DDQ is stronger than in *o*-benzyne, however. This interaction energy can be quantified by the singlet biradical stabilization energy, 2.01 eV, or by the heat of hydrogenation (1 equiv.), −323.5 kJ mol^{-1}. Various electronic states of 2,3-DDQ prove problematic for certain levels of theory, indicating the importance of surveying multiple correlated methods in the study of biradical structure and reactivity.

Acknowledgements

As a scientist, I have been fortunate in the number of superb collaborators with whom I've had the opportunity to interact. Bob Squires was one of those collaborators and more than that, he was a good friend. As I worked on this project and interesting results developed, my excitement was constantly tempered by the sorrow and frustration that I could no longer call and discuss the details with the one individual best suited to *share* that excitement (and no doubt to tell me how to improve the science, too). I will forever miss Bob's keen chemical insights, his endless energy and enthusiasm, and his dry sense of humor. I am grateful to be able to dedicate this paper to him.

High-performance vector and parallel computing resources made available by the Minnesota Supercomputer Institute and the University of Minnesota-IBM Shared Research Project, respectively. Funding was provided by the National Science Foundation and the Alfred P. Sloan Foundation. I benefited from discussions with Professor Steven Kass.

References

1 R. W. Hoffmann, *Dehydrobenzene and Cycloalkynes*, Academic Press, New York, 1967.
2 T. L. Gilchrist and C. W. Rees, *Carbenes, Nitrenes and Arynes*, Nelson, London, 1969.
3 C. Wentrup, *Reactive Molecules*, Wiley, New York, 1984, p. 288.
4 R. H. Levin, in *Reactive Intermediates*, M. Jones and R. Moss, Eds., Wiley, New York, 1985, vol. 3, p. 1.
5 R. Hoffmann, A. Imamura and W. J. Hehre, *J. Am. Chem. Soc.*, 1968, **90**, 1499.
6 T. Kauffmann and R. Wirthwein, *Angew. Chem., Int. Ed. Engl.*, 1971, **10**, 20.
7 M. R. Bryce and J. M. Vernon, *Adv. Heterocycl. Chem.*, 1981, **28**, 183.
8 M. A. Bennett and H. P. Schwemlein, *Angew. Chem., Int. Ed. Engl.*, 1989, **28**, 1296.
9 G. E. Davico, R. L. Schwartz, T. M. Ramond and W. C. Lineberger, *J. Am. Chem. Soc.*, 1999, **121**, 6047.
10 J. C. Rienstra-Kiracofe, D. E. Graham and H. F. Schaefer, III, *Mol. Phys.*, 1998, **94**, 767.
11 T. H. Dunning, *J. Chem. Phys.*, 1989, **90**, 1007.
12 A. D. Becke, *Phys. Rev. A*, 1988, **38**, 3098.
13 J. P. Perdew, K. Burke and Y. Wang, *Phys. Rev. B*, 1996, **54**, 6533.
14 K. Andersson, P.-Å. Malmqvist, B. O. Roos, A. J. Sadlej and K. Wolinski, *J. Phys. Chem.*, 1990, **94**, 5483.
15 K. Andersson and B. O. Roos, *Int. J. Quantum. Chem.*, 1993, **45**, 591.
16 K. Andersson, M. R. A. Blomberg, M. P. Fülscher, G. Karlström, V. Kellö, R. Lindh, P.-Å. Malmqvist, J. Noga, J. Olsen, B. O. Roos, A. J. Sadlej, P. E. M. Siegbahn, M. Urban and P.-O. Widmark, *MOLCAS-3*, University of Lund, Sweden, 1994.
17 J. Cizek, *Adv. Chem. Phys.*, 1969, **14**, 35.
18 G. D. Purvis and R. J. Bartlett, *J. Chem. Phys.*, 1982, **76**, 1910.
19 J. Gauss and C. Cremer, *Chem. Phys. Lett.*, 1988, **150**, 280.
20 K. Raghavachari, G. W. Trucks, J. A. Pople and M. Head-Gordon, *Chem. Phys. Lett.*, 1989, **157**, 479.
21 N. Handy, J. A. Pople, M. Head-Gordon, K. Raghavachari and G. W. Trucks, *Chem. Phys. Lett.*, 1989, **164**, 185.
22 J. F. Stanton, *Chem. Phys. Lett.*, 1997, **281**, 130.
23 C. J. Cramer, *J. Am. Chem. Soc.*, 1998, **120**, 6261.
24 M. H. Lim, S. E. Worthington, F. J. Dulles and C. J. Cramer, in *Density-Functional Methods in Chemistry*, B. B. Laird, R. B. Ross and T. Ziegler, Eds., American Chemical Society, Washington, DC, 1996, vol. 629, p. 402.
25 M. J. Frisch, G. W. Trucks, H. B. Schlegel, P. M. W. Gill, B. G. Johnson, M. A. Robb, J. R. Cheeseman, T. Keith, G. A. Petersson, J. A. Montgomery, K. Raghavachari, M. A. Al-Laham, V. G. Zakrzewski, J. V. Ortiz, J. B. Foresman, J. Cioslowski, B. B. Stefanov, A. Nanayakkara, M. Challacombe, C. Y. Peng, P. Y. Ayala, W. Chen, M. W. Wong, J. L. Andres, E. S. Replogle, R. Gomperts, R. L. Martin, D. J. Fox, J. S. Binkley, D. J. Defrees, J. Baker, J. P. Stewart, M. Head-Gordon, C. Gonzalez and J. A. Pople, *Gaussian 94 RevD.1*; Gaussian Inc., Pittsburgh, PA, 1995.
26 P. G. Wenthold, R. R. Squires and W. C. Lineberger, *J. Am. Chem. Soc.*, 1998, **120**, 5279.
27 C. J. Cramer, J. J. Nash and R. R. Squires, *Chem. Phys. Lett.*, 1997, **277**, 311.
28 E. Kraka, D. Cremer, G. Bucher, H. Wandel and W. Sander, *Chem. Phys. Lett.*, 1997, **268**, 313.
29 C. J. Cramer and S. Debbert, *Chem. Phys. Lett.*, 1998, **287**, 320.
30 B. Engels and M. Hanrath, *J. Am. Chem. Soc.*, 1998, **120**, 6356.
31 P. R. Schreiner, *J. Am. Chem. Soc.*, 1998, **120**, 4184.
32 H. F. Bettinger, P. v. R. Schleyer and H. F. Schaefer, III, *J. Am. Chem. Soc.*, 1999, **121**, 2829.
33 C. J. Cramer, *Org. Lett.*, 1999, **1**, 215.
34 E. Kraka and D. Cremer, *J. Am. Chem. Soc.*, 1994, **116**, 4929.

35 R. R. Squires and C. J. Cramer, *J. Phys. Chem. A*, 1998, **102**, 9072.
36 T. Heinis, S. Chowdhury, S. L. Scott and P. Kebarle, *J. Am. Chem. Soc.*, 1988, **110**, 400.
37 C. J. Cramer and R. R. Squires, *J. Phys. Chem. A*, 1997, **101**, 9191.
38 S. G. Wierschke, J. J. Nash and R. R. Squires, *J. Am. Chem. Soc.*, 1993, **115**, 11958.
39 P. G. Wenthold, S. G. Wierschke, J. J. Nash and R. R. Squires, *J. Am. Chem. Soc.*, 1994, **116**, 7378.
40 J. B. Pedley, R. D. Naylor and S. P. Kirby, *Thermochemical Data of Organic Compounds*, Chapman and Hall, New York, 1986.
41 E. Ruiz, D. Salahub and A. Vela, *J. Am. Chem. Soc.*, 1995, **117**, 1141.
42 Y. Zhang and W. Yang, *J. Chem. Phys.*, 1998, **109**, 2604.
43 P. Hohenberg and W. Kohn, *Phys. Rev. B*, 1964, **3**, 864.
44 O. Gunnarsson and B. I. Lundqvist, *Phys. Rev. B*, 1976, **13**, 4274.
45 B. A. Smith and C. J. Cramer, *J. Am. Chem. Soc.*, 1996, **118**, 5490.
46 M. B. Sullivan, K. R. Brown, C. J. Cramer and D. G. Truhlar, *J. Am. Chem. Soc.*, 1998, **120**, 11778.
47 J. D. Watts and R. J. Bartlett, *Chem. Phys. Lett.*, 1996, **258**, 581.

Paper 9/03116B